ORIGINAL ARTICLE

Enhanced osteoinductive capacity of poly(lactic-co-glycolic) acid and biphasic ceramic scaffolds by embedding simvastatin

Mariane B. Sordi[1,2] · Raissa B. Curtarelli[1,2] · Iara F. Mantovani[3] · Anderson C. Moreira[3] · Celso P. Fernandes[3] · Ariadne C. C. Cruz[1,2] · Ricardo S. Magini[3]

Abstract

Objectives This study evaluated the effect of embedding simvastatin (SIM) on the osteoinductive capacity of PLGA + HA/ βTCP scaffolds in stem cells from human exfoliated deciduous teeth (SHED).

Materials and methods Scaffolds were produced by PLGA solvent dissolution, addition of HA/βTCP, solvent evaporation, and leaching of sucrose particles to impart porosity. Biphasic ceramic particles (70% HA/30% βTCP) were added to the PLGA in a 1:1 (w:w) ratio. Scaffolds with SIM received 1% (w:w) of this medication. Scaffolds were synthesized in a disc-shape and sterilized by ethylene oxide. The experimental groups were (G1) PLGA + HA/βTCP and (G2) PLGA + HA/βTCP + SIM in non-osteogenic culture medium, while (G3) SHED and (G4) MC3T3-E1 in osteogenic culture medium were the positive control groups. The release profile of SIM from scaffolds was evaluated. DNA quantification assay, alkaline phosphatase activity, osteocalcin and osteonectin proteins, extracellular calcium detection, von Kossa staining, and X-ray microtomography were performed to assess the capacity of scaffolds to induce the osteogenic differentiation of SHED.

Results The release profile of SIM followed a non-liner sustained-release rate, reaching about 40% of drug release at day 28. Additionally, G2 promoted the highest osteogenic differentiation of SHED, even when compared to the positive control groups.

Conclusions In summary, the osteoinductive capacity of poly(lactic-co-glycolic) acid and biphasic ceramic scaffolds was expressively enhanced by embedding simvastatin.

Clinical relevance Bone regeneration is still a limiting factor in the success of several approaches to oral and maxillofacial surgeries, though tissue engineering using mesenchymal stem cells, scaffolds, and osteoinductive mediators might collaborate to this topic.

Keywords Bone regeneration · Simvastatin · Mesenchymal stem cells · Scaffolds · Osteogenic differentiation

✉ Ariadne C. C. Cruz
ariadne.cruz@ufsc.br; ariadnecruz@hotmail.com

1 Department of Dentistry, Center for Research On Dental Implants (CEPID), Federal University of Santa Catarina, Florianopolis, Brazil

2 Department of Microbiology, Immunology, and Parasitology, Laboratory of Applied Virology (LVA), Federal University of Santa Catarina, Florianopolis, Brazil

3 Department of Mechanical Engineering, Laboratory of Porous Media and Thermophysical Properties (LMPT), Federal University of Santa Catarina, Florianopolis, Brazil

Introduction

Dimensional limitations of alveolar bone due to the resorption and remodeling after exodontia, infection, periodontal disease, or trauma may complicate, or prevent, the rehabilitation with implant-supported prostheses. Tissue engineering studies of new approaches, including scaffolds, signaling molecules, and mesenchymal stem cells (MSC), have been widely applied and promising results are obtained [1–13].

Osteoconductive scaffolds may be used as a framework to allow cell and vessel invasion, facilitating, or even accelerating, bone regeneration. In implant dentistry, scaffolds are not intended to act as a permanent bone substitute [14] but provide a temporary structure with similar properties to those of the host bone. The combination of poly(lactic-co-glycolic)

acid (PLGA) polymer with hydroxyapatite (HA) and β-tricalcium phosphate (βTCP) ceramics synergize to generate a more favorable biomaterial. The beneficial characteristics of the individual substances, such as the release of calcium and phosphate ions from the biphasic ceramics, and the improvement of mechanical resistance to compression, adequate degradation rate [15–22], and incorporation of bioactive substances into the polymeric scaffolds, synergize to form a controlled-release system for osteoinduction [23, 24].

Drug delivery systems with osteoinductive substances may improve the performance of the scaffolds. Statins, specifically simvastatin (SIM), are potent reducers of endogenous cholesterol synthesis and are widely used to prevent coronary disease and atherosclerosis. Their effect involves an increase of the bone morphogenetic protein (BMP) expression levels in bone cells and the stimulus of new bone formation [25–29]. SIM applied alone, i.e., with no carrier, demonstrated osteogenic effect over undifferentiated cells in vitro [30–35]. However, the clinical success of SIM in bone regeneration is related to a slow and controlled release process since high local dosages induce an exacerbated inflammatory response [16, 29, 36] due to the cytotoxicity and the reduction of cholesterol production in cell membranes [7, 28]. Consequently, to reach a sustained SIM release to the applied site, a carrier (normally a three-dimensional material or scaffold) is recommended. Additionally, the use of SIM leads to a reduced risk of clinical side-effects compared to growth factors or gene therapies [30]. Therefore, this study evaluated the effect of embedding SIM on the osteoinductive capacity of PLGA + HA/βTCP scaffolds in stem cells from human exfoliated deciduous teeth (SHED).

Methods

Samples preparation

Scaffolds were produced with PLGA and biphasic ceramic composed of HA and βTCP obtained by PLGA solvent dissolution, the addition of HA/βTCP, solvent evaporation, and leaching of sucrose particles, as previously described [17, 18]. Briefly, PLGA composite was a 1:1 blend of polylactic acid (Resomer LT 706S) lactide-co-glycolide (Resomer LG 824S) (Evonik Boehringer Ing. Pharma GmbH&Co. KG, Germany). Biphasic ceramic (Genphos, Genius with HA and βTCP in the ratio 70/30, Baumer, São Paulo, Brazil) were added to the polymer blend in a 1:1 ratio. For samples containing SIM (≥ 97%, high-performance liquid chromatography (HPLC) grade, solid M = 418.57, Sigma-Aldrich, St. Louis, Missouri, USA), the drug was added to the polymer blend at 10 mg/g. Samples were sectioned into discs of 5 mm diameter and 1.5 mm height and sterilized by ethylene oxide.

SIM release

Samples were incubated in 5 mL of phosphate-buffered saline (PBS), pH 7.4, in a 37 °C and 5% CO_2 incubator chamber for up to 90 days. At different time intervals, 200 µL of the solution was collected and the absorbance was measured on a UV–vis spectrophotometer at 238 nm (TECAN, Zürich, Switzerland). The collected PBS was quantified and returned to the original solution at the end of each reading. The standard curve was obtained from known concentrations of SIM in acetonitrile and used to quantify the loaded SIM and its release from the samples. To analyze the SIM release profile, the SIM concentration was re-dimensioned by dividing the absolute amount of SIM released at time t (Mt) by the amount of SIM at infinity ($M\infty$), which was the equilibrated concentration obtained at the end of the 90-day experimental period, since it depends not only on how much drug has been added but also on the solubility of the material. The models were evaluated based on the correlation coefficient (r^2) [17].

MSC cultures

To determine the scaffold capacity to induce the osteogenic differentiation of SHED, cell cultures were conducted using 96-well plates with 2×10^4 cells per well at 37 °C and 5% CO_2. Cell culture media for SHED were Dulbecco's Modified Eagle's Medium (DMEM, Gibco, Thermo Fischer Scientific, Waltham, USA) with 10% fetal bovine serum (FBS, Invitrogen, Thermo Fischer Scientific, Waltham, USA) (regular medium) or DMEM with 10% FBS, 1% penicillin–streptomycin (PS, Invitrogen, Thermo Fischer Scientific, Waltham, USA), 50 mM ascorbate-2-phosphate (Sigma-Aldrich, St. Louis, USA), 10 mM β-glycerophosphate (Sigma-Aldrich, St. Louis, USA), and 0.1 mM dexamethasone (Sigma-Aldrich, St. Louis, USA) (osteogenic medium). Alpha-Modified Minimum Essential Medium (α-MEM, Nutricell, SP, Brazil) with 10% FBS, 1% PS, 50 mM ascorbate-2-phosphate, and 10 mM β-glycerophosphate (osteogenic medium) was used for pre-osteoblasts MC3T3-E1 subclone 4 (ATCC, Virginia, USA). Two experimental groups were determined: (G1) PLGA + HA/βTCP and (G2) PLGA + HA/βTCP + SIM, applying SHED in a regular medium. The average mass of scaffolds for the experimental was 0.02 g. Additionally, two positive control groups were established: (G3) SHED and (G4) MC3T3-E1 in an osteogenic culture medium. All experiments were performed in triplicate at predetermined experimental times.

DNA quantification assay

On days 3, 7, 14, 21, and 28, cell proliferation was assessed through the content of DNA in the groups using Quant-iT TM PicoGreen® dsDNA Reagent (P7589, Invitrogen, Thermo Fisher Scientific, CA, USA). Analyses were performed according to Sordi et al. (2021) [37] and readings were carried out on a fluorescence spectrophotometer (SpectraMax M2e, Molecular Devices, CA, USA) at 480/520 nm (Ex/Em).

Osteogenic differentiation assays

Alkaline phosphatase (ALP) activity was measured using the Alkaline Phosphatase Fluorimetric Assay Kit (Abnova, Taipei, Taiwan). Analyses were performed according to the manufacturer's recommendations and readings were performed on a fluorescence spectrophotometer (SpectraMax M2e, Molecular Devices, CA, USA) at 360/440 nm (Ex/Em). Experimental times were on days 3, 7, and 14. Data were normalized against DNA content.

Extracellular calcium quantification was measured using QuantiChrom Calcium Assay Kit (Bioassay Systems, California, USA). Analyses were performed according to the manufacturer's recommendations and absorbance was recorded using a spectrophotometer (SpectraMax M2e, Molecular Devices, CA, USA) at 612 nm. Calcium quantifications were performed on days 7, 14, 21, and 28.

Quantification of osteocalcin and osteonectin proteins was measured using the Quantikine ELISA Human Osteocalcin Immunoassay and Human SPARC Immunoassay (R&D Systems, Minnesota, USA), respectively [38, 39]. Analyses were performed according to the manufacturer's recommendations at 450 nm with wavelength correction set to 540 nm (SpectraMax M2e, Molecular Devices, CA, USA). Evaluations were performed on days 14 and 21.

Nodules of mineralization were marked using von Kossa staining. For that, cells were fixed with 4% paraformaldehyde for 60 min at room temperature. Then, cells were washed with ultrapure water, covered with 1% silver nitrate solution, and incubated for 30 min, protected from light. Counterstaining with 0.1% eosin solution in ethanol was performed and the results were observed and photographed from a light microscope [40]. Analyses were performed on day 28.

X-ray microtomography (µCT)

Images of scaffold microstructure were obtained using high-resolution three-dimensional X-ray microtomography (Versa XRM-500, ZEISS/Xradia, Oberkochen, Germany). The scanning conditions were the same for all samples: X-ray tube at 50 kV/4 W, no filter for beam hardening effect,

$0.4\times$ optical lens, 0.225° angular step, and 3 s exposure time. The resulting images had a spatial resolution (voxel size) of 9.40–9.44 µm [17]. The µCT images were processed using Avizo 8.0 (Thermo Fisher Scientific, Waltham, Massachusetts, USA). Evaluations were performed using the same samples before cell seeding (day 0) and after 28 days of SHED culture.

Statistical analyses

Data were analyzed using the GraphPad Software (San Diego, USA) through two-way analyses of variances (ANOVA) followed by Tukey's multiple comparison test for DNA, ALP, calcium, osteocalcin, and osteonectin data. Values of $p < 0.05$ were considered statistically significant. These analyses were performed for each group, and experimental time, independently.

Results

SIM release

SIM was slowly and gradually released from scaffolds until the day 90 of the experiment with no latency period (Fig. 1). On day 3 of the experiment, 10% of the equilibrated concentration (M∞) was already released from samples, while on day 14 up to day 28, about 30% to 40% of the M∞ were released. After the 90-day period, the release curve still exhibited an increasing behavior, without reaching an equilibrium (Fig. 1a). The release profile of SIM followed a non-liner sustained-release rate decreasing up to day 21, meaning that up to day 28 it is found the strongest rate release of SIM (Fig. 1b).

DNA quantification

Regarding DNA quantification assay (Fig. 2a), G1 revealed an increase in the DNA content from day 3 to day 21, followed by a decrease to day 28. The groups that were possibly differentiating (G2 and G3) remained mainly stable over the time (no statistical differences from day 3 to day 28), while G4 presented an increase in the DNA content from day 3 to day 28.

Osteogenic differentiation

For ALP activity ($p < 0.0001$, Fig. 2b), extracellular calcium ($p < 0.0001$, Fig. 2c), osteocalcin ($p < 0.0001$, Fig. 2d), and osteonectin ($p < 0.0001$, Fig. 2e), G2 produced notably higher results than the other groups, including the control groups, at all the experimental times. Interestingly, there were an increase on osteocalcin ($p < 0.0001$) and a decrease
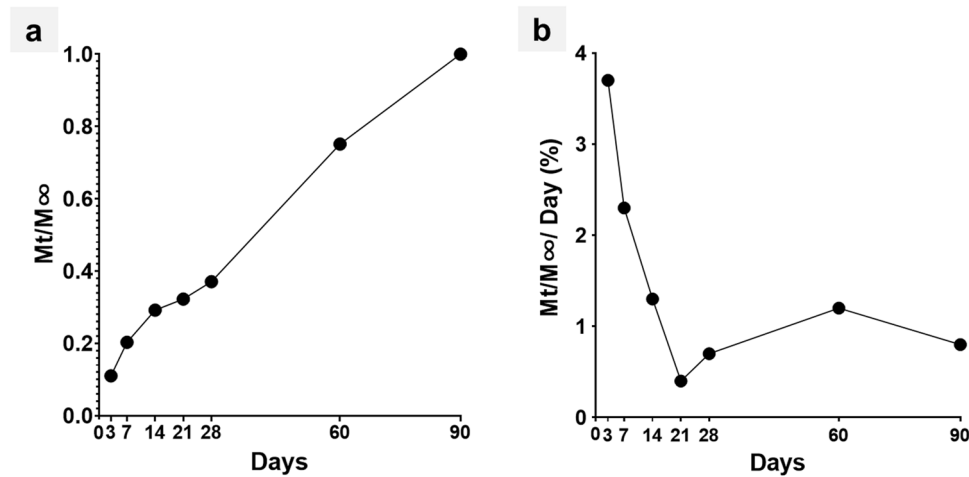
Fig. 1 a Simvastatin release from PLGA + HA/βTCP + SIM scaffolds for up to 90 days in phosphate-buffered saline. Calculations were carried out by dividing the absolute amount of simvastatin released at time t (Mt) by the amount of simvastatin at infinity (M∞), which was the equilibrated concentration obtained at the end of the 90-day experimental period. **b** Simvastatin release rate from PLGA + HA/ βTCP + SIM scaffolds for up to 90 days. Data was calculated by using the SIM release from the previously measured data (Mt/M∞) expressed as percentage (at $T=0$ 0% is released and $T=90$ 100% is released). This was divided by the number of days between each period to show the % of total SIM released per day (%/day)
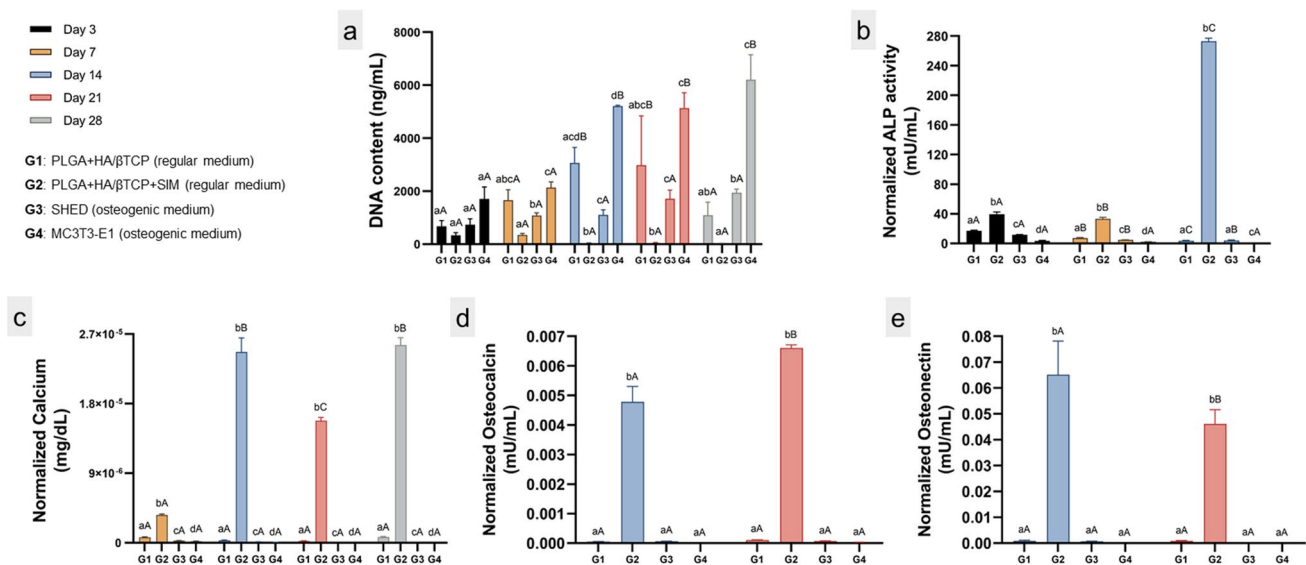

Fig. 2 a DNA content assay by PicoGreen® reagent to determine the cell proliferation on days 3, 7, 14, 21, and 28. The DNA content data was used to normalize ALP activity, extracellular free calcium, and osteocalcin and osteonectin proteins. **b** Alkaline phosphatase (ALP) activity on days 3, 7, and 14. **c** Extracellular free calcium on days 7, 14, 21, and 28. **d** ELISA Human Osteocalcin Immunoassay on days 14 and 21, and **e** ELISA Human Osteonectin Immunoassay on days 14 and 21. Different lower-case letters refer to a significant difference (ANOVA/Tukey test, $p < 0.05$) among groups at the same experimental time. Different capital letters indicate significant differences (ANOVA/Tukey test, $p < 0.05$) among the experimental times for the same group

on osteonectin ($p = 0.001$) levels from day 14 to day 21 for G2 (Fig. 2d and e, respectively).

Regarding the mineralization of extracellular matrix (ECM, Fig. 3), G2 and G3 presented high concentrations of mineralized nodules but in a different pattern of deposition. G4 showed less nodules of mineralization than G2 and G3, while G1 showed the least mineralization of the ECM.
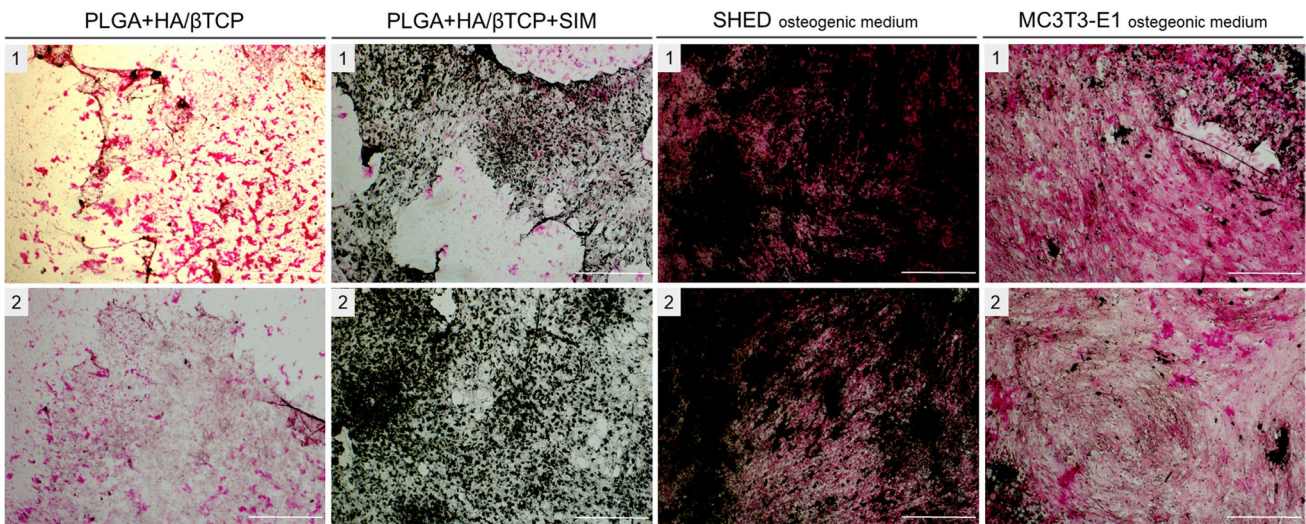
Fig. 3 Von Kossa staining to detect mineralization nodules (colored in brown/black) on day 28. The figure above shows two of the three samples performed. Scale bars represent 500 μm

X-ray microtomography (μCT)

For X-ray microtomography (Fig. 4a-h), gray level 3D images were filtered with "Non-Local Means Denoising" [41] "Unsharp Mask" [42] tools using the AVIZO software and then they were segmented into dense (HA/βTCP), matrix (PLGA), and pore phases. The segmentation process was carried out based on gray level histogram analysis by choosing a threshold that best separates the analyzed phases. After the segmentation, cylindrical volumes of interest (VOI) were outlined for porosity and phase fractions determinations. It can be observed that porosity and matrix phases were similar for both scaffolds and for both experimental times (days 0 and 28); however, the dense phase was more contrasting for PLGA+HA/βTCP+SIM (Fig. 4i). The binary VOIs were modeled into 3D network images. The
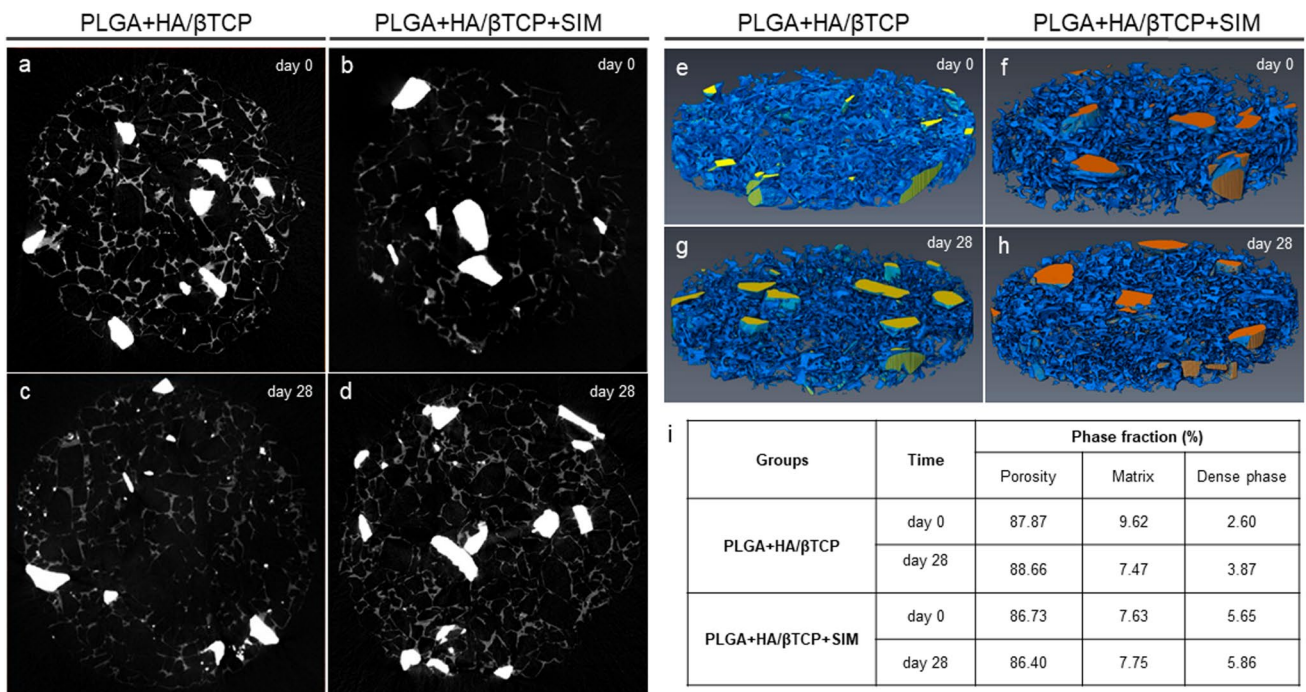

Groups	Time	Phase fraction (%)		
		Porosity	Matrix	Dense phase
PLGA+HA/βTCP	day 0	87.87	9.62	2.60
	day 28	88.66	7.47	3.87
PLGA+HA/βTCP+SIM	day 0	86.73	7.63	5.65
	day 28	86.40	7.75	5.86

Fig. 4 X-ray microtomography (**a–d**) and 3D network images (**e–h**) obtained before SHED seeding on day 0 and after 28 days of cell culture on the scaffolds. The scaffolds porosity, matrix, and dense phases are presented in the table (**i**)

porosity of about 85 to 90% and the well dispersion of the biphasic ceramic particles across the scaffolds indicate that the samples were successfully produced.

Discussion

Bone regeneration is still a limiting factor in the success of several approaches to oral and maxillofacial surgeries, though tissue engineering using MSC, scaffolds, and osteoinductive mediators might provide a solution [8, 11, 43]. Suitable scaffolds for this purpose continue to be investigated. In our previous research, we developed a biomaterial with adequate structural, chemical, thermal, and biological properties for bone tissue engineering applications [17, 18]. Thus, with the promising results of our aforementioned data, herein we aimed to evaluate the osteogenic capacity of PLGA + HA/βTCP scaffolds embedding SIM in vitro. In summary, we observed that the PLGA + HA/βTCP + SIM group demonstrated results notably higher than the other groups regarding ALP activity, calcium quantification, and osteocalcin and osteonectin proteins quantifications at all the experimental times, even when compared to the positive control groups. Concerning the ECM mineralization analyzed by von Kossa, SHED cultured in osteogenic medium and PLGA + HA/βTCP + SIM group presented high concentrations of ECM mineralization with the nodules deposited in different patterns. Considering the relevance of obtaining a controlled-release system for osteoinduction that has adequate mechanical and chemical properties, degradation rate, biocompatibility, and osteoinduction capacity, these findings are extremely promising for oral and maxillofacial applications. Additionally, the fabrication technique of the proposed delivery system is simple, affordable, and can be mass produced. Also, the raw materials are synthetic and are established in the scientific literature. These factors all contribute to the likelihood that the proposed delivery system could be feasible for use in clinical application [14, 15, 20, 21]. Furthermore, SIM has a good safety profile when applied in appropriate dosages [18, 27, 29, 30, 36, 44]. In addition, additive manufacturing such as bioprinting, using the materials applied herein, could be utilized for the personalized bioprinting of scaffolds for bone defects detected from computed tomography exams.

A deep understanding of the molecular regulatory networks of osteoblast proliferation and differentiation is fundamental to effectively develop biomaterials for bone regeneration [29]. In this context, the methodology of this study was designed with an emphasis on the osteogenic differentiation pathway [44]. The cell commitment to osteogenesis occurs within the first week of osteogenic stimulation when the osteoprogenitor cells enter an early stage of active proliferation followed by a stage of reduction in proliferation

due to cell maturation [45, 46]. This initial commitment can be verified by DNA content assay, where increasing DNA is related to more cells, i.e. cell proliferation. Our findings revealed that the groups under strong differentiation stimulus (G2 and G3) remained mainly stable over time.

The early osteogenic markers are present in the first 7 to 14 days of the osteogenic differentiation process and include type 1 collagen and alkaline phosphatase [44, 46]. When preosteoblasts begin their maturation, there is an increase in the alkaline phosphatase activity, which provides phosphate ions for the initial mineralization of the ECM and, consequently, calcium in the extracellular media increases its concentration [44–46]. Such events were proven in the present study by the sharp increase in both alkaline phosphatase activity and concentration of extracellular free calcium on day 14 of the performed analyses, which was more significant in the PLGA + HA/βTCP + SIM scaffolds (G2). Additionally, the release profile of SIM followed a non-liner sustained-release rate. Even at its fastest release rate, in the beginning days, the DNA content and ALP activity results during this period suggested the cells were viable and the SIM released dose was adequate.

Osteocalcin, osteonectin, and osteopontin are considered intermediate proteins in the osteogenic differentiation fate, typically present from days 14 to 21 of cell maturation. Those proteins act on the mineralization of the immature ECM [46]. Herein, the quantifications of osteocalcin and osteonectin validate the alkaline phosphatase and calcium findings, since PLGA + HA/βTCP + SIM scaffolds (G2) promoted the highest protein levels on days 14 and 21 compared to the other groups, including the positive controls. These results are in agreement with other studies that also evaluated SIM playing a role in the osteoinduction of MSCs for bone regeneration [30, 44]. In the late stage of the osteogenic differentiation pathway, mature differentiated cells mineralize the ECM by trapping the free calcium [44, 46]. We have demonstrated by von Kossa staining the presence of mineralized nodules in the ECM of the SHED control group and the group under stimulation of PLGA + HA/βTCP + SIM scaffolds, validating the enhanced osteogenic capacity from embedding SIM [40, 47, 48]. The reduction of calcium on the extracellular media followed by its increase from day 21 to day 28 may be related to the trapping of the free calcium used to mineralize the ECM, which was already mineralized on day 28. The μCT images show that only minor changes in the matrix shape of the scaffolds were observed over a period of 28 days of the experiment, which might be related to the controlled and prolonged release of SIM from the scaffolds, which is favorable for bone regeneration purposes, as already presented in our previous studies [17, 18].

The use of SIM for bone tissue regeneration or in the treatment of other bone diseases was already extensively studied [4–7, 27–29, 36, 44, 48]. SIM seems to act on bone

regeneration through an increase in BMP-2 expression level [25–29, 44]. The primary pathway of osteogenesis includes the BMP-2/Smads signaling pathway, in which BMP-2 triggers the osteogenic signal by phosphorylating Smads, and then mediates the expressions of the genes associated with osteoblast differentiation, such as alkaline phosphatase and osteocalcin [29, 48, 49]. However, the detailed mechanism by which SIM acts on osteogenic differentiation of MSC remains unknown while the signaling pathways that modulate the cell differentiation are considered potential targets of SIM activity [48]. Besides the BMP-2/Smads, Hedgehog and MAPK signaling pathways may be related to the SIM-induced osteogenic differentiation of MSC [44, 48]. Nevertheless, it is important to mention that this is an in vitro study. Further studies on the details of the mechanisms of SIM in the osteogenic differentiation pathway, as well as in vivo and clinical trials, should be performed to confirm our data.

Conclusions

In summary, PLGA + HA/βTCP + SIM scaffolds promoted the highest osteogenic differentiation of SHED. Therefore, the present study revealed the outstanding results of embedding SIM into PLGA and biphasic ceramic scaffolds to differentiate SHED into the osteoblastic lineage. This is mainly due to the development of a biomaterial with adequate structural, chemical, thermal, and biological properties for bone tissue engineering applications, in addition to the successful incorporation method, adequate dosage, and prolonged release of SIM from the scaffolds, which enhanced osteogenic differentiation of dental-derived mesenchymal stem cells.

Declarations

Ethical approval This article does not contain any studies with human participants or animals performed by any of the authors.

Informed consent For this type of study, formal consent is not required.

Conflict of interest The authors declare no competing interests.

References

1. Hämmerle CH (2000) Karring T (1998) Guided bone regeneration at oral implant sites. Periodontol 17:151–175. https://doi.org/10.1111/j.1600-0757.1998.tb00132.x
2. Buser D, Dula K, Hess D et al (2000) (1999) Localized ridge augmentation with autografts and barrier membranes. Periodontol 19:151–163. https://doi.org/10.1111/j.1600-0757.1999.tb00153.x
3. Sakai VT, Zhang Z, Dong Z et al (2010) SHED differentiate into functional odontoblasts and endothelium. J Dent Res 89:791–796. https://doi.org/10.1177/0022034510368647
4. Zhou Y, Ni Y, Liu Y et al (2010) The role of simvastatin in the osteogenesis of injectable tissue-engineered bone based on human adipose-derived stromal cells and platelet-rich plasma. Biomaterials 31:5325–5335. https://doi.org/10.1016/j.biomaterials.2010.03.037
5. Wadagaki R, Mizuno D, Yamawaki-Ogata A et al (2011) Osteogenic induction of bone marrow-derived stromal cells on simvastatin-releasing, biodegradable, nano- to microscale fiber scaffolds. Ann Biomed Eng 39:1872–1881. https://doi.org/10.1007/s10439-011-0327-0
6. Qi Y, Zhao T, Yan W et al (2013) Mesenchymal stem cell sheet transplantation combined with locally released simvastatin enhances bone formation in a rat tibia osteotomy model. Cytotherapy 15:44–56. https://doi.org/10.1016/j.jcyt.2012.10.006
7. Mendes Junior D, Domingues JA, Hausen MA et al (2017) Study of mesenchymal stem cells cultured on a poly(lactic-co-glycolic acid) scaffold containing simvastatin for bone healing. J Appl Biomater Funct Mater 15:e133–e141. https://doi.org/10.5301/jabfm.5000338
8. Ciapetti G, Granchi D, Baldini N (2012) The combined use of mesenchymal stromal cells and scaffolds for bone repair. Curr Pharm Des 18:1796–1820
9. Liu J, Ruan J, Weir MD, et al (2019) Periodontal bone-ligament-cementum regeneration via scaffolds and stem cells. Cells 8:. https://doi.org/10.3390/cells8060537
10. Fahimipour F, Dashtimoghadam E, Mahdi Hasani-Sadrabadi M et al (2019) Enhancing cell seeding and osteogenesis of MSCs on 3D printed scaffolds through injectable BMP2 immobilized ECM-Mimetic gel. Dent Mater 35:990–1006. https://doi.org/10.1016/j.dental.2019.04.004
11. Steffens D, Braghirolli DI, Maurmann N, Pranke P (2018) Update on the main use of biomaterials and techniques associated with tissue engineering. Drug Discov Today 23:1474–1488. https://doi.org/10.1016/j.drudis.2018.03.013
12. Beck JD, Philips K, Moss K et al (2020) Advances in precision oral health. Periodontol 2000(82):268–285. https://doi.org/10.1111/prd.12314
13. Saito H, Aichelmann-Reidy MB (2000) Oates TW (2020) Advances in implant therapy in North America: improved outcomes and application in the compromised dentition. Periodontol 82:225–237. https://doi.org/10.1111/prd.12319
14. Fisher PD, Venugopal G, Milbrandt TA et al (2015) Hydroxyapatite-reinforced in situ forming PLGA systems for intraosseous injection. J Biomed Mater Res A 103:2365–2373. https://doi.org/10.1002/jbm.a.35375
15. Kim J, McBride S, Tellis B et al (2012) Rapid-prototyped PLGA/β-TCP/hydroxyapatite nanocomposite scaffolds in a rabbit femoral defect model. Biofabrication 4:025003. https://doi.org/10.1088/1758-5082/4/2/025003
16. Encarnação IC, Xavier CCF, Bobinski F et al (2016) Analysis of bone repair and inflammatory process caused by simvastatin combined with PLGA+HA+βTCP scaffold. Implant Dent 25:140–148. https://doi.org/10.1097/ID.0000000000000359

17. Encarnação IC, Sordi MB, Aragones Á et al (2019) Release of simvastatin from scaffolds of poly(lactic-co-glycolic) acid and biphasic ceramic designed for bone tissue regeneration. J Biomed Mater Res Part B Appl Biomater. https://doi.org/10.1002/jbm.b.34311

18. Sordi MB, Cabral da Cruz AC, Aragones Á et al (2020) PLGA+HA/βTCP scaffold incorporating simvastatin: a promising biomaterial for bone tissue engineering. J Oral Implantol. https://doi.org/10.1563/aaid-joi-D-19-00148

19. Guan L, Davies JE (2004) Preparation and characterization of a highly macroporous biodegradable composite tissue engineering scaffold. J Biomed Mater Res A 71:480–487. https://doi.org/10.1002/jbm.a.30173

20. Huang YX, Ren J, Chen C et al (2008) Preparation and properties of poly(lactide-co-glycolide) (PLGA)/ nano-hydroxyapatite (NHA) scaffolds by thermally induced phase separation and rabbit MSCs culture on scaffolds. J Biomater Appl 22:409–432. https://doi.org/10.1177/0885328207077632

21. Tayton E, Purcell M, Aarvold A et al (2014) A comparison of polymer and polymer-hydroxyapatite composite tissue engineered scaffolds for use in bone regeneration. An in vitro and in vivo study. J Biomed Mater Res A 102:2613–2624. https://doi.org/10.1002/jbm.a.34926

22. Roy A, Jhunjhunwala S, Bayer E et al (2016) Porous calcium phosphate-poly (lactic-co-glycolic) acid composite bone cement: a viable tunable drug delivery system. Mater Sci Eng C Mater Biol Appl 59:92–101. https://doi.org/10.1016/j.msec.2015.09.081

23. Yang F, Cui W, Xiong Z et al (2006) Poly(l, l-lactide-co-glycolide)/tricalcium phosphate composite scaffold and its various changes during degradation in vitro. Polym Degrad Stab 91:3065–3073. https://doi.org/10.1016/j.polymdegradstab.2006.08.008

24. Boerckel JD, Kolambkar YM, Dupont KM et al (2011) Effects of protein dose and delivery system on BMP-mediated bone regeneration. Biomaterials 32:5241–5251. https://doi.org/10.1016/j.biomaterials.2011.03.063

25. Mundy G, Garrett R, Harris S et al (1999) Stimulation of bone formation in vitro and in rodents by statins. Science 286:1946–1949. https://doi.org/10.1126/science.286.5446.1946

26. Maeda T, Matsunuma A, Kurahashi I et al (2004) Induction of osteoblast differentiation indices by statins in MC3T3-E1 cells. J Cell Biochem 92:458–471. https://doi.org/10.1002/jcb.20074

27. Gentile P, Nandagiri VK, Daly J et al (2016) Localised controlled release of simvastatin from porous chitosan-gelatin scaffolds engrafted with simvastatin loaded PLGA-microparticles for bone tissue engineering application. Mater Sci Eng C Mater Biol Appl 59:249–257. https://doi.org/10.1016/j.msec.2015.10.014

28. Yamashita M, Otsuka F, Mukai T et al (2008) Simvastatin antagonizes tumor necrosis factor-alpha inhibition of bone morphogenetic proteins-2-induced osteoblast differentiation by regulating Smad signaling and Ras/Rho-mitogen-activated protein kinase pathway. J Endocrinol 196:601–613. https://doi.org/10.1677/JOE-07-0532

29. Feng C, Xiao L, Yu J-C et al (2020) Simvastatin promotes osteogenic differentiation of mesenchymal stem cells in rat model of osteoporosis through BMP-2/Smads signaling pathway. Eur Rev Med Pharmacol Sci 24:434–443. https://doi.org/10.26355/eurrev_202001_19943

30. Huang Y, Lin Y, Rong M et al (2019) 20(S)-hydroxycholesterol and simvastatin synergistically enhance osteogenic differentiation of marrow stromal cells and bone regeneration by initiation of Raf/MEK/ERK signaling. J Mater Sci Mater Med 30:87. https://doi.org/10.1007/s10856-019-6284-0

31. Niu J, Ding G, Zhang L (2015) Effects of simvastatin on the osteogenic differentiation and immunomodulation of bone marrow mesenchymal stem cells. Mol Med Rep 12:8237–8240. https://doi.org/10.3892/mmr.2015.4476

32. So-Hyun S, Il-Kyu L, Jee-Won L et al (2009) Simvastatin induces osteogenic differentiation and suppresses adipogenic differentiation in primarily cultured human adipose-derived stem cells. Biomol Ther 17:353–361. https://doi.org/10.4062/biomolther.2009.17.4.353

33. Chuang S-C, Chen C-H, Fu Y-C et al (2015) Estrogen receptor mediates simvastatin-stimulated osteogenic effects in bone marrow mesenchymal stem cells. Biochem Pharmacol 98:453–464. https://doi.org/10.1016/j.bcp.2015.09.018

34. Jin Y-Q, Zhang L, Tian F-M et al (2011) Effects of simvastatin on Wnt and bone morphogenetic protein 2 signaling pathway during osteoblast differentiation of bone marrow stromal cells. J Clin Rehab Tissue Eng Res 15:6732–6736. https://doi.org/10.3969/j.issn.1673-8225.2011.36.019

35. Tai I-C, Wang Y-H, Chen C-H et al (2015) Simvastatin enhances Rho/actin/cell rigidity pathway contributing to mesenchymal stem cells' osteogenic differentiation. Int J Nanomedicine 10:5881–5894. https://doi.org/10.2147/IJN.S84273

36. Park J-B (2009) The use of simvastatin in bone regeneration. Med Oral Patol Oral Cir Bucal 14:e485-488

37. Sordi MB, Curtarelli RB, da Silva IT et al (2021) Effect of dexamethasone as osteogenic supplementation in in vitro osteogenic differentiation of stem cells from human exfoliated deciduous teeth. J Mater Sci Mater Med 32:1. https://doi.org/10.1007/s10856-020-06475-6

38. Almela T, Al-Sahaf S, Bolt R et al (2018) Characterization of multilayered tissue-engineered human alveolar bone and gingival mucosa. Tissue Eng Part C Methods 24:99–107. https://doi.org/10.1089/ten.TEC.2017.0370

39. Cakal OT, Efeoglu C, Bozkurt E (2018) The evaluation of peri-implant sulcus fluid osteocalcin, osteopontin, and osteonectin levels in peri-implant diseases. J Periodontol 89:418–423. https://doi.org/10.1002/JPER.17-0475

40. Cruz ACC, de Souza Cardozo FTG, de Souza Magini R, Simões CMO (2019) Retinoic acid increases the effect of bone morphogenetic protein type 2 on osteogenic differentiation of human adipose-derived stem cells. J Appl Oral Sci 27:e20180317. https://doi.org/10.1590/1678-7757-2018-0317

41. Buades A, Coll B, Morel J-M (2011) Non-local means denoising. Image Processing On Line 1:. https://doi.org/10.5201/ipol.2011.bcm_nlm

42. Sheppard AP, Sok RM, Averdunk H (2004) Techniques for image enhancement and segmentation of tomographic images of porous materials. Physica A 339:145–151. https://doi.org/10.1016/j.physa.2004.03.057

43. Sheikh Z, Sima C, Glogauer M (2015) Bone replacement materials and techniques used for achieving vertical alveolar bone augmentation. Materials (Basel) 8:2953–2993. https://doi.org/10.3390/ma8062953

44. Shao P-L, Wu S-C, Lin Z-Y, et al (2019) Alpha-5 integrin mediates simvastatin-induced osteogenesis of bone marrow mesenchymal stem cells. Int J Mol Sci 20:. https://doi.org/10.3390/ijms20030506

45. Infante A, Rodríguez CI (2018) Osteogenesis and aging: lessons from mesenchymal stem cells. Stem Cell Res Ther 9:244. https://doi.org/10.1186/s13287-018-0995-x

46. Paiva KBS, Granjeiro JM (2017) Chapter six - matrix metalloproteinases in bone resorption, remodeling, and repair. In: Khalil RA (ed) Progress in Molecular Biology and Translational Science (vol. 148). Academic Press, Massachusetts, pp 203–303

47. Rimando MG, Wu H-H, Liu Y-A et al (2016) Glucocorticoid receptor and Histone deacetylase 6 mediate the differential effect of dexamethasone during osteogenesis of mesenchymal stromal cells (MSCs). Nat Sci Rep https://doi.org/10.1038/srep37371

48. Chi B, Fan X, Li Z et al (2019) Identification of Gli1-interacting proteins during simvastatin-stimulated osteogenic differentiation

of bone marrow mesenchymal stem cells. J Cell Biochem 120:18979–18994. https://doi.org/10.1002/jcb.29221

49. Yamachika E, Tsujigiwa H, Shirasu N et al (2009) Immobilized recombinant human bone morphogenetic protein-2 enhances the phosphorylation of receptor-activated Smads. J Biomed Mater Res A 88:599–607. https://doi.org/10.1002/jbm.a.31833